TECHNICAL MEMORANDUM

X - 47

STATIC STABILITY AND CONTROL CHARACTERISTICS OF AN AIRPLANE MODEL WITH TAIL SURFACES OUTBOARD OF THE WING TIPS AT A MACH NUMBER OF 2.01

By Cornelius Driver and M. Leroy Spearman

Langley Research Center
Langley Field, Va.

NATIONAL AERONAUTICS AND SPACE ADMINISTRATION

WASHINGTON September 1959

NATIONAL AERONAUTICS AND SPACE ADMINISTRATION

TECHNICAL MEMORANDUM X-47

STATIC STABILITY AND CONTROL CHARACTERISTICS OF AN AIRPLANE MODEL WITH TAIL SURFACES OUTBOARD OF THE WING TIPS AT A MACH NUMBER OF 2.01*

By Cornelius Driver and M. Leroy Spearman

SUMMARY

An investigation has been conducted in the Langley 4- by 4-foot supersonic pressure tunnel at a Mach number of 2.01 to determine the static stability and control characteristics of an airplane configuration with tail surfaces outboard of the wing tips. Complete model tests were made with two sizes of horizontal tails. In addition, tests were made of various combinations of component parts.

The results indicated that values of maximum trimmed lift-drag ratio were relatively insensitive to stability level up to a static margin of 26.5 percent. The highest value of trimmed lift-drag ratio obtained was about 6.55. All configurations indicated a positive dihedral effect, and the complete configuration indicated positive static directional stability at the approximate angle of attack for the maximum trimmed lift-drag ratio.

INTRODUCTION

Recent investigations have indicated that airplane configurations employing horizontal tail surfaces outboard and rearward of the wing tips should provide an improvement in performance characteristics over more conventional designs. Low-speed studies of some models with tail surfaces outboard of the wing tips and a discussion of some of the basic concepts and applications of these designs are presented in reference 1. Wind-tunnel studies at supersonic speeds of some models with tail surfaces outboard of the wing tips are presented in references 2 and 3. Further refinements have subsequently been made to the configuration reported in reference 3, and tests of the revised model are presented herein at a Mach number of 2.01. The model was tested primarily in pitch with various

*Title, Unclassified.

control deflections for two sizes of horizontal tails although some limited sideslip data were also obtained. In addition, some results for various combinations of model component parts were obtained.

COEFFICIENTS AND SYMBOLS

The results are referred to the body axis system except for the lift and drag coefficients, which are referred to the wind axis system. The moment reference point is at a longitudinal station corresponding to the quarter chord of the mean geometric chord.

The coefficients and symbols are defined as follows:

C_L lift coefficient, $\frac{\text{Lift}}{qS}$

C_D drag coefficient, $\frac{\text{Drag}}{qS}$

C_m pitching-moment coefficient, $\frac{\text{Pitching moment}}{qS\bar{c}}$

C_l rolling-moment coefficient, $\frac{\text{Rolling moment}}{qSb}$

C_n yawing-moment coefficient, $\frac{\text{Yawing moment}}{qSb}$

C_Y side-force coefficient, $\frac{\text{Side force}}{qS}$

q free-stream dynamic pressure

S area of wing including fuselage intercept plus horizontal tail, sq in.

$\bar{c}$ mean geometric chord of wing plus horizontal tail, in.

b span of wing plus horizontal tail, in.

α angle of attack, deg

β angle of sideslip, deg

i_t horizontal tail control deflection (measured with respect to outer body center line), deg

ϵ	effective angle of downwash, deg
L/D	lift-drag ratio, C_L/C_D
C_{n_β}	directional-stability parameter
C_{l_β}	effective-dihedral parameter
$\frac{\partial C_m}{\partial C_L}$	longitudinal-stability parameter
C_{L_α}	lift-curve slope
$\frac{\partial \epsilon}{\partial \alpha}$	variation of effective downwash angle with angle of attack

Subscripts:

max	maximum
o	value at zero lift
trim	value measured at $C_m = 0$

Model component designations:

B	body
H	horizontal tail
W	wing
V	vertical tail
O	outer body
E	engine pack

MODELS AND APPARATUS

Details of the model are shown in figure 1 and the geometric characteristics are presented in table I. The model consisted of a

body having a semielliptical cross section with the wing mounted essentially flush with the lower side of the body. Beneath the wing-body was a simulated six-engine pack with a vertical two-dimensional split inlet ducted to four exits. Outer bodies were attached to the wing tips for the purpose of supporting the vertical and horizontal tails. The rear portions of the outer bodies were deflected 1.5° inward and 3° upward. Thus with respect to the body reference axis, the vertical tails were mounted with the leading edge deflected 1.5° outward, and with respect to the wing-chord plane, the horizontal tails (for $i_t = 0$) were mounted with the trailing edge deflected 3° upward. Two sizes of horizontal tails were tested (designated small and large). The tails were all-movable with the hinge line at 50 percent of the root chord.

The model was mounted in the tunnel on a remote-controlled rotary sting, and force and moment measurements were made with the use of a six-component internal strain-gage balance.

TEST CONDITIONS AND CORRECTIONS

The tests for this investigation were conducted in the Langley 4- by 4-foot supersonic pressure tunnel at a Mach number of 2.01, a stagnation pressure of 10 lb/sq in., and a stagnation temperature of 110° F. The stagnation dewpoint was maintained sufficiently low (-25° F or less) to prevent condensation effects in the test section. The Reynolds number, based on $\bar{c}$ with the small horizontal tail, was 3.3×10^6. Limited data were obtained for a Reynolds number of 6.6×10^6. However, since a comparison of these data with those obtained at a Reynolds number of 3.3×10^6 indicated little significant difference (fig. 2), the remainder of the data were obtained at the lower Reynolds number.

Tests were made through an angle-of-attack range of about -4° to 10° at $\beta = 0^\circ$ and through a sideslip range from -2° to 6° at angles of attack of 0° and 4°.

The angles of attack were determined directly by optical means and required no correction, whereas the angles of sideslip were determined indirectly and have been corrected for the deflection of the balance and sting under load. The base pressure was measured, and the drag force was adjusted to correspond to a base pressure equal to free-stream static pressure. The drag has been corrected to account for the internal flow through the engine pack.

DISCUSSION

Longitudinal Characteristics

Effect of component parts.- The aerodynamic characteristics in pitch for various combinations of component parts for the model with the small horizontal tail are presented in figure 3. The addition of the outer bodies provides a small increase in lift-curve slope as a result of the end-plate effect on the wing and a small increase in longitudinal stability. In addition, the outer bodies cause a slight increase in minimum drag and a decrease in the maximum value of L/D.

The addition of the horizontal tail results in an increase in lift-curve slope because of the effective increase in aspect ratio. The horizontal tail, of course, provides positive longitudinal stability, and because of the 3° upward deflection of the outer bodies, a positive increment of the $C_{m,o}$ results. A tendency toward reduced stability is indicated for the complete configuration at lift coefficients above about 0.3. The addition of the horizontal tail causes an increase in minimum drag, but because of a decrease in the drag due to lift, the maximum value of L/D is increased. The reduction in drag due to lift is partly a result of the increase in aspect ratio of the wing-tail combination and partly a result of the fact that the horizontal tail is located in a region of upwash from the wing. An analysis of the results for the complete configuration indicates a drag-due-to-lift factor $\Delta C_D/C_L{}^2$ of 0.436 as compared with a value of 0.478 which is indicated by the reciprocal of the lift-curve slope $\left(1/57.3C_{L_\alpha}\right)$. The fact that the drag-due-to-lift factor is lower than would be expected on the basis of the lift-curve slope is an indication of the favorable effect of upwash at the horizontal tail. A similar effect would be expected for the configuration with the large horizontal tail.

The addition of the vertical tails has little effect other than to cause a slight increase in minimum drag and a slight reduction in the maximum value of L/D.

Effect of horizontal tail deflection.- The effects of horizontal tail deflection on the aerodynamic characteristics in pitch are shown in figure 4 for the small horizontal tail and in figure 5 for the large horizontal tail. Deflection of either tail provides a uniform variation of pitching moment throughout the lift range. However, because of the reduced stability at higher lifts, the maximum lift obtainable before encountering control reversal is about 0.3.

Although deflection of the horizontal tail causes an increase in minimum drag, the drag-due-to-lift factor is improved so that the maximum value of L/D is not drastically reduced with increased tail deflection.

The pitching-moment results for the various tail deflections as well as those for the tail off have been used to determine the experimental values of effective downwash (fig. 6). At the intersections of the tail-off curve with the tail-on curves (where the tail provides no pitching moment), it is assumed that the tail is alined with the local stream direction and hence the downwash angle can be determined from the relation $\epsilon = \alpha + i_t$. The resulting values (fig. 6) indicate a negative variation of ϵ with α, or an effective upwash flow at the tail. The value of $\partial\epsilon/\partial\alpha$ is about -1.1 for either the small or the large tail. Although the results (fig. 6) indicate a positive value of ϵ at $\alpha = 0^\circ$, it should be pointed out that the flow angle is referred to the chord plane of the horizontal tail which is inclined -3° to the free-stream direction.

Longitudinal trim characteristics.- The maximum trimmed values of L/D as a function of stability level $\partial C_m/\partial C_L$ (measured near zero lift) are shown in figure 7 for both tail sizes. These values were obtained from the data presented in figures 4 and 5 for various arbitrary stability levels. At stability levels for which the values of maximum L/D occurred for control deflections other than those tested, the values were interpolated by assuming a linear variation of pitching moment with control deflection.

The maximum trimmed values of L/D are relatively insensitive to stability level over a reasonably large range (static margin up to 26.5 percent). The highest values of trimmed L/D obtained were about 6.55 for both tails, and these values occurred at stability levels of $\partial C_m/\partial C_L = -0.14$ for the small tail and of $\partial C_m/\partial C_L = -0.165$ for the large tail.

Lateral Stability

The aerodynamic characteristics in sideslip for various combinations of component parts for the configuration with the small horizontal tail are presented in figure 8 for angles of attack of 0° and 4°. The addition of the outer bodies to the wing-body-engine configuration provides a stabilizing increment in directional stability. The possibility of obtaining this stabilizing increment in directional stability by use of outer bodies was discussed in reference 4 and is an effect that might be expected to increase with increasing angle of attack.

The addition of the vertical tail provides a substantial increment of directional stability that is reduced slightly by the addition of the horizontal tail at $\alpha = 4^\circ$ (fig. 8(b)). However, the complete model indicates positive static directional stability at the approximate angle of attack for maximum L/D ($\alpha = 4^\circ$).

All configurations displayed a positive dihedral effect $(-C_{l_\beta})$. The increment in C_{l_β} provided by the vertical tail at $\alpha = 4^\circ$ is somewhat reduced by the presence of the horizontal tail. This effect is apparently related to the interference flow field of the vertical tail on the horizontal tail as was pointed out in reference 2.

The effect of horizontal tail size on the sideslip derivatives (fig. 9) is limited to only a slight increase in $-C_{l_\beta}$ as the tail size is increased.

The effects of horizontal tail deflection on the sideslip characteristics (figs. 10 and 11) were quite small and consisted primarily of a slight increase in C_{n_β} with positive deflection and a slight decrease in C_{n_β} with negative deflection at $\alpha = 4^\circ$. These effects are characteristic of low tail configurations. (See ref. 4.) The effects of horizontal tail deflection might be expected to increase with increasing deflection; however, the -6° deflection is well beyond that required for trimming at the maximum L/D.

CONCLUDING REMARKS

An investigation has been conducted in the Langley 4- by 4-foot supersonic pressure tunnel at a Mach number of 2.01 to determine the stability and control characteristics of an airplane configuration with tail surfaces outboard of the wing tips. The results of the investigation indicated that maximum trimmed values of lift-drag ratio were relatively insensitive to stability level up to a static margin of 26.5 percent. The highest value of trim lift-drag ratio obtained was about 6.55. All configurations indicated a positive dihedral effect, and the complete model indicated positive static directional stability at the approximate angle of attack for the maximum trimmed lift-drag ratio.

Langley Research Center,
National Aeronautics and Space Administration,
Langley Field, Va., April 29, 1959.

REFERENCES

1. Sleeman, William C., Jr.: Preliminary Study of Airplane Configurations Having Tail Surfaces Outboard of the Wing Tips. NACA RM L58B06, 1958.

2. Spearman, M. Leroy, and Robinson, Ross B.: Aerodynamic Characteristics of a Canard and an Outboard-Tail Airplane Model at a Mach Number of 2.01. NACA RM L58B07, 1958.

3. Church, James D., Hayes, William C., Jr., and Sleeman, William C., Jr.: Investigation of Aerodynamic Characteristics of an Airplane Configuration Having Tail Surfaces Outboard of the Wing Tips at Mach Numbers of 2.30, 2.97, and 3.51. NACA RM L58C25, 1958.

4. Spearman, M. Leroy: Some Factors Affecting the Static Longitudinal and Directional Stability Characteristics of Supersonic Aircraft Configurations. NACA RM L57E24a, 1957.

TABLE I.- GEOMETRIC CHARACTERISTICS OF MODEL

Wing alone:			
Area, sq in.			300
Span, in.			16.432
Mean geometric chord, in.			18.5
Aspect ratio			0.9
Taper ratio			0.665
Airfoil section			2.5 percent thick hexagonal
Twist, deg			0
Dihedral, deg			0
Leading-edge sweep, deg			60
Trailing-edge sweep, deg			40
Vertical tail (each semispan):			
Area, sq in.			20
Span, in.			3.868
Mean geometric chord, in.			5.79
Aspect ratio			0.748
Taper ratio			0.25
Airfoil section			2.5 percent thick double wedge
Incidence (toe out), deg			1.5
Leading-edge sweep, deg			55
Trailing-edge sweep, deg			-10
Outer body:			
Length, in.			27.5
Fineness ratio			20.14
Body:			
Length, in.			39.50
Fineness ratio			15.65
Wing plus horizontal tail:		Small tail	Large tail
Area, sq in.		360	374.99
Span, in.		27.53	28.92
Mean geometric chord, in.		16.43	16.15
Aspect ratio		2.11	2.23
Taper ratio		0.0986	0.1095
Horizontal tail (each semispan):			
Area, sq in.		30	37.495
Span, in.		5.549	6.244
Mean geometric chord, in.		6.055	6.728
Aspect ratio		1.03	1.04
Taper ratio		0.25	0.25
Airfoil section		2.5 percent thick hexagonal	2.5 percent thick hexagonal
Twist, deg		0	0
Dihedral, deg		0	0
Leading-edge sweep, deg		60	60
Trailing-edge sweep, deg		29.38	29.38

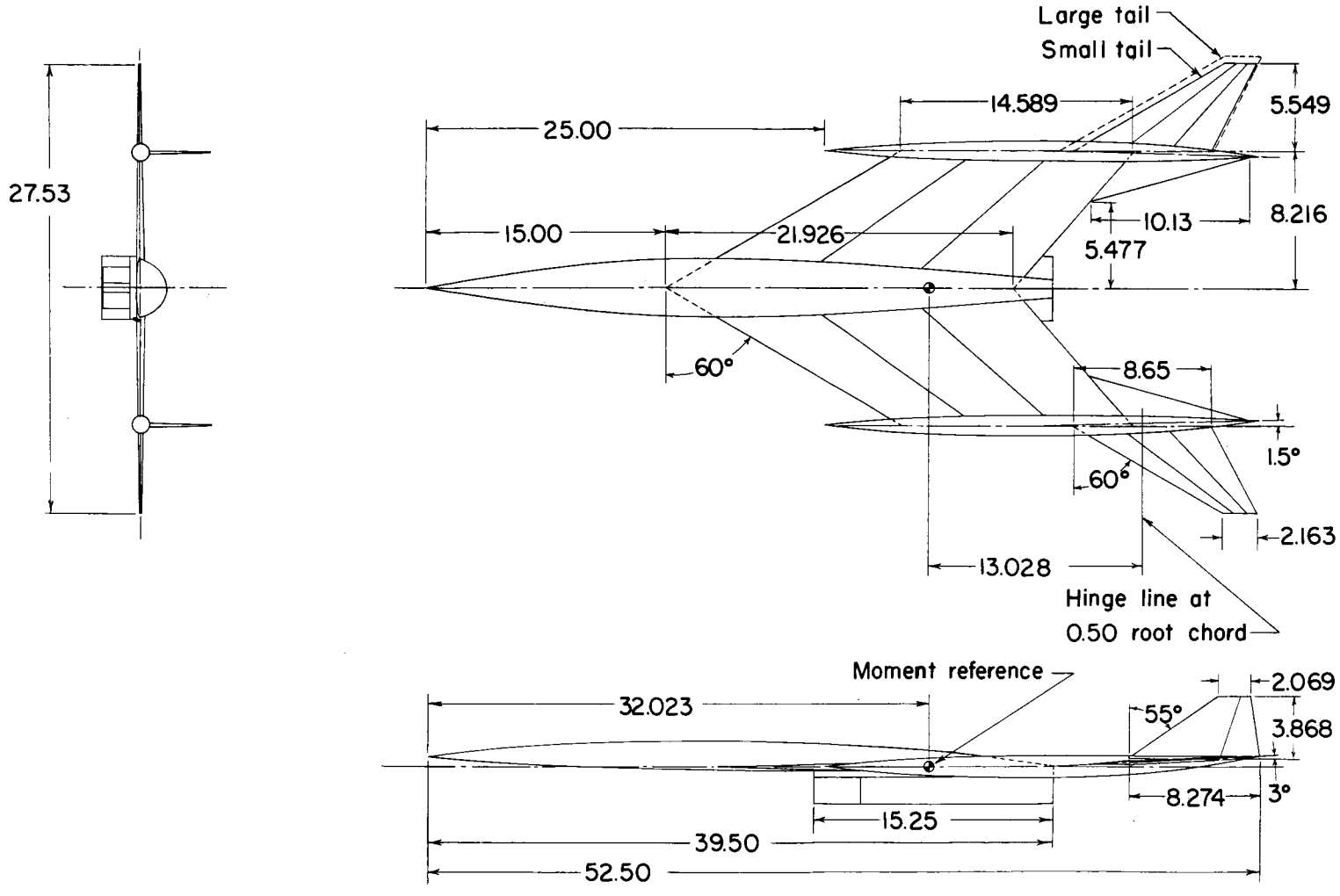

Figure 1.- Details of model. All linear dimensions in inches.

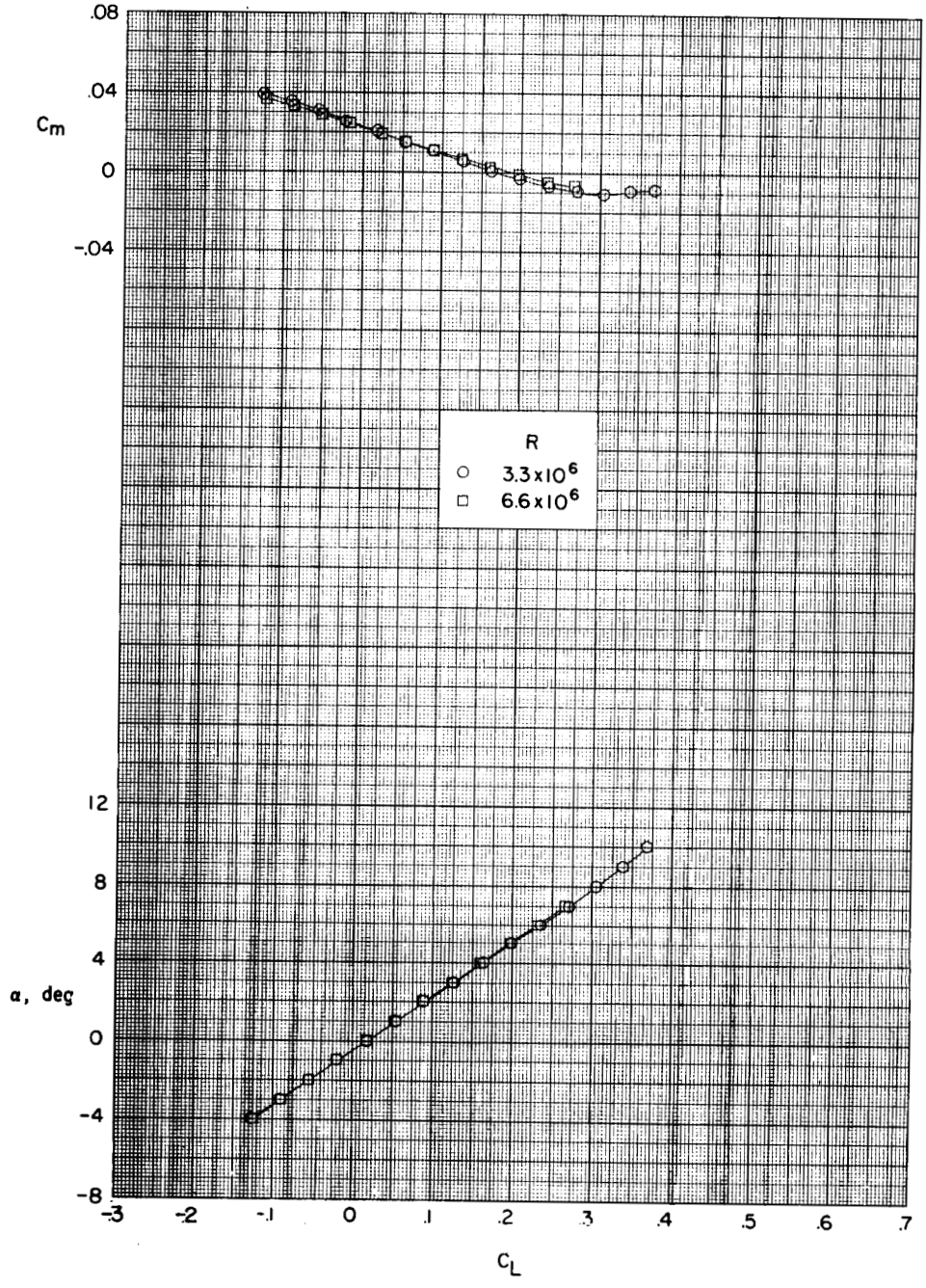

(a) Variation of pitching-moment coefficient and angle of attack with lift coefficient.

Figure 2.- Effect of Reynolds number on aerodynamic characteristics in pitch for complete model with small horizontal tail $(i_t = 0^\circ)$.

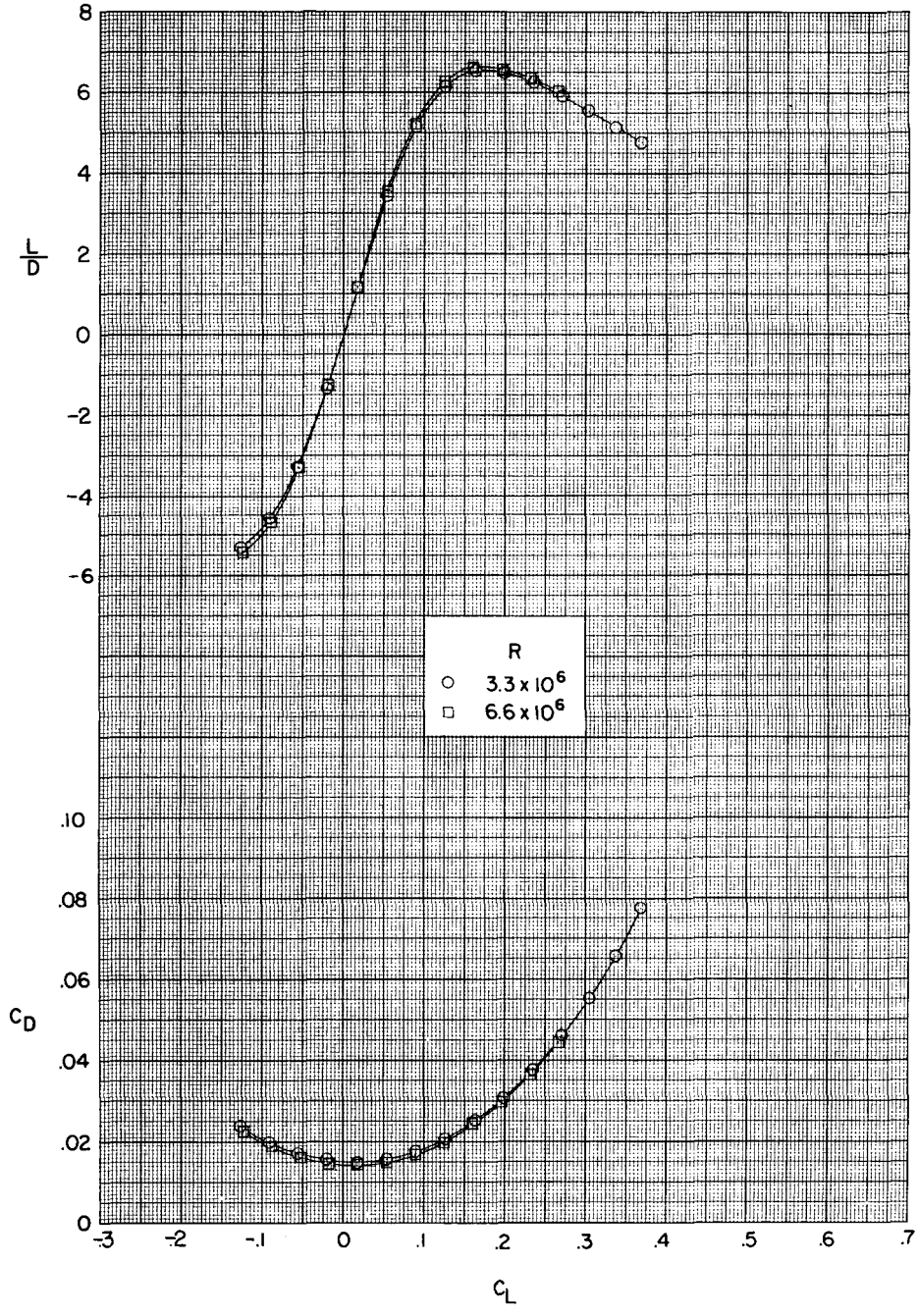

(b) Variations of lift-drag ratio and drag coefficient with lift coefficient.

Figure 2.- Concluded.

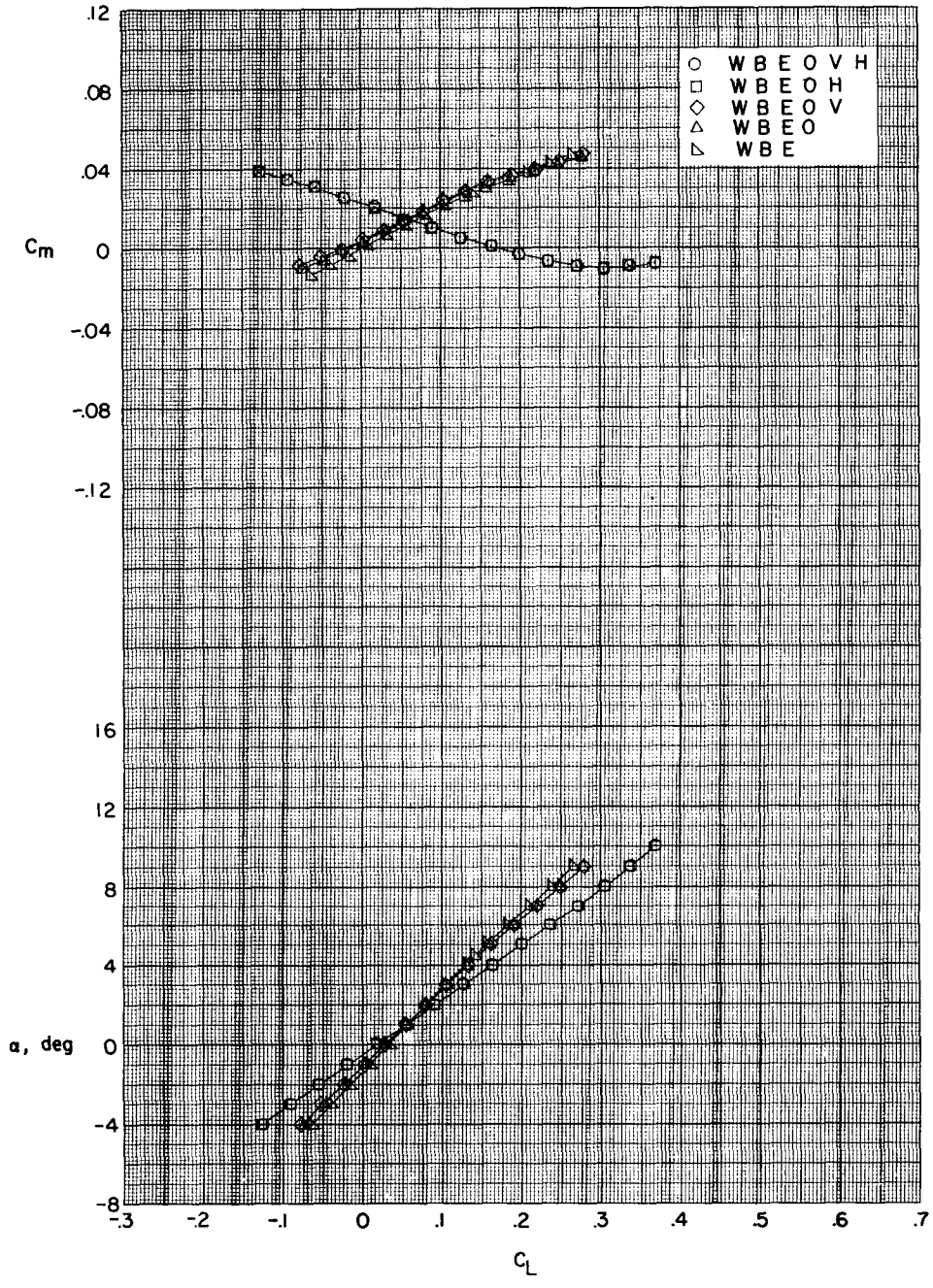

(a) Variation of pitching-moment coefficient and angle of attack with lift coefficient.

Figure 3.- Aerodynamic characteristics in pitch for various combinations of component parts with small horizontal tail $\left(i_t = 0^\circ\right)$.

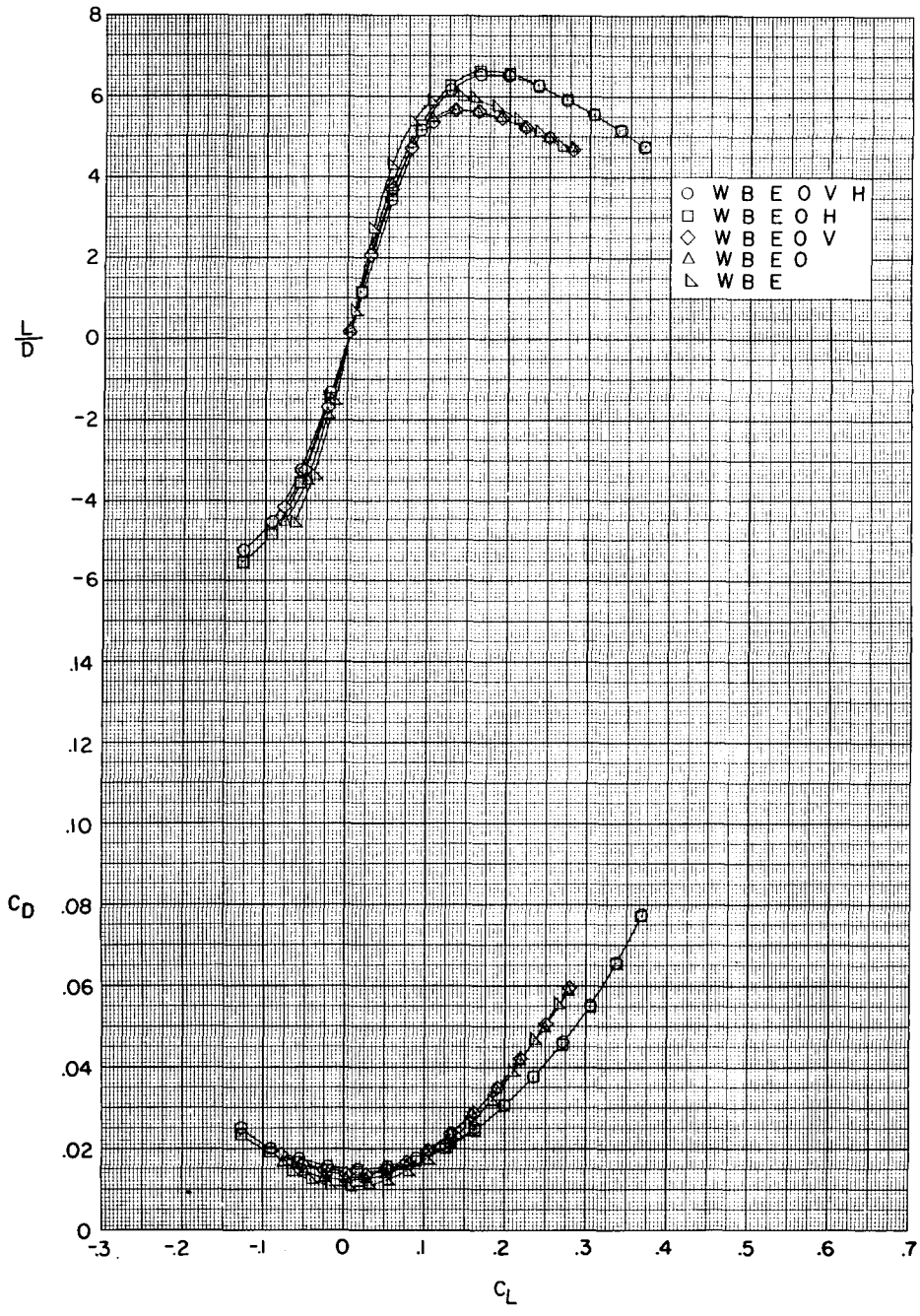

(b) Variation of lift-drag ratio and drag coefficient with lift coefficient.

Figure 3.- Concluded.

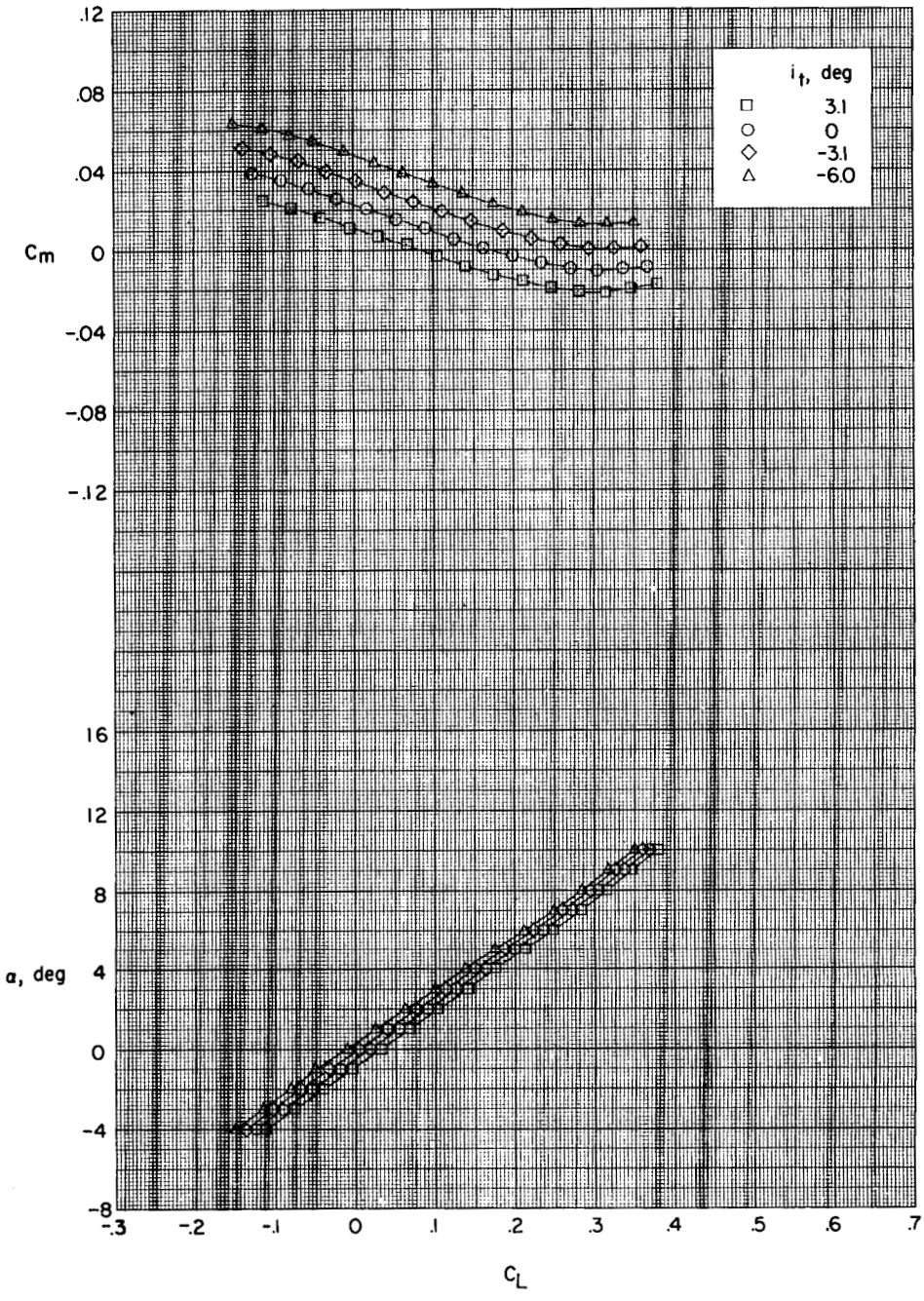

(a) Variation of pitching-moment coefficient and angle of attack with lift coefficient.

Figure 4.- Effect of horizontal tail deflection on aerodynamic characteristics in pitch for complete model with small horizontal tail.

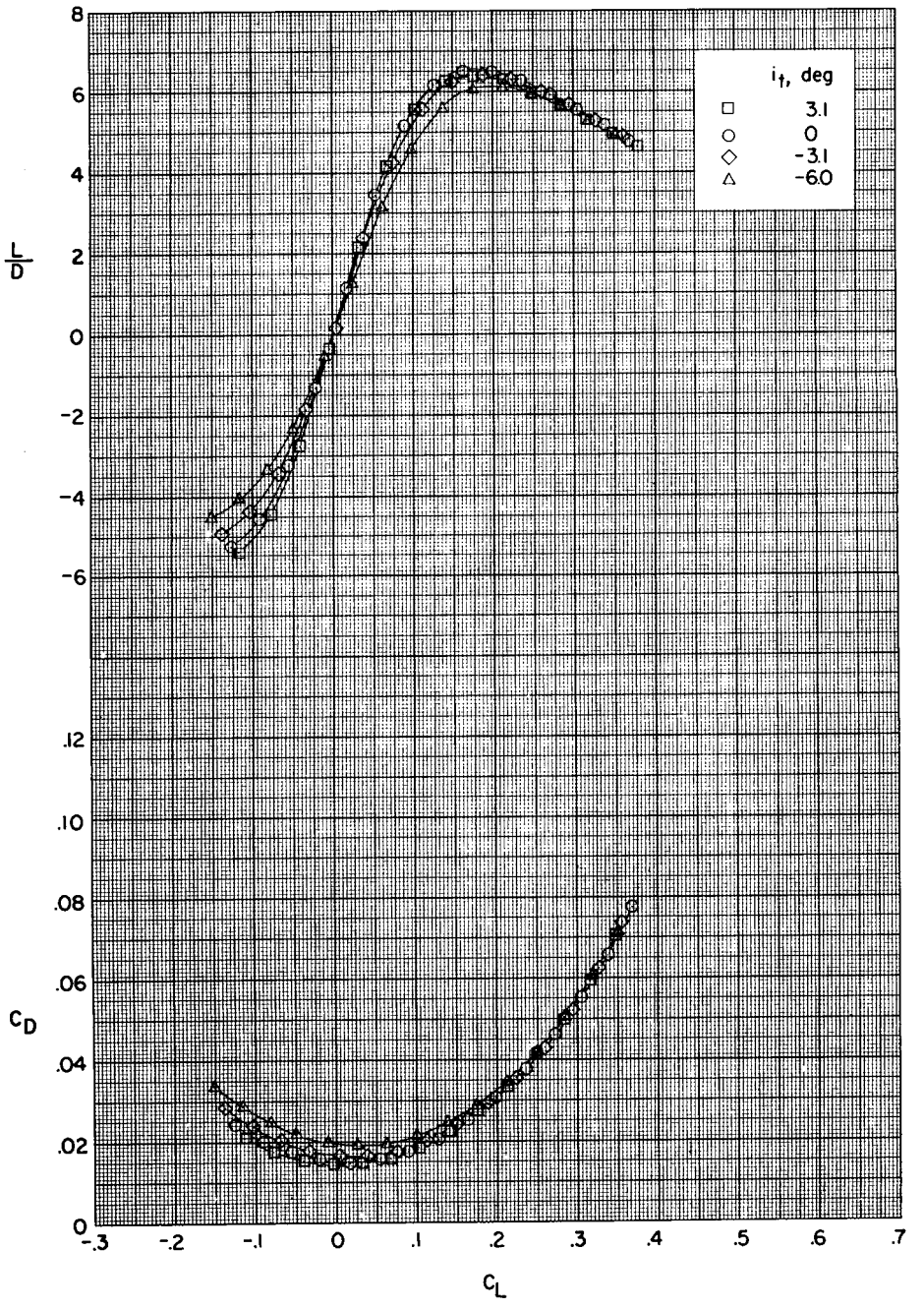

(b) Variation of lift-drag ratio and drag coefficient with lift coefficient.

Figure 4.- Concluded.

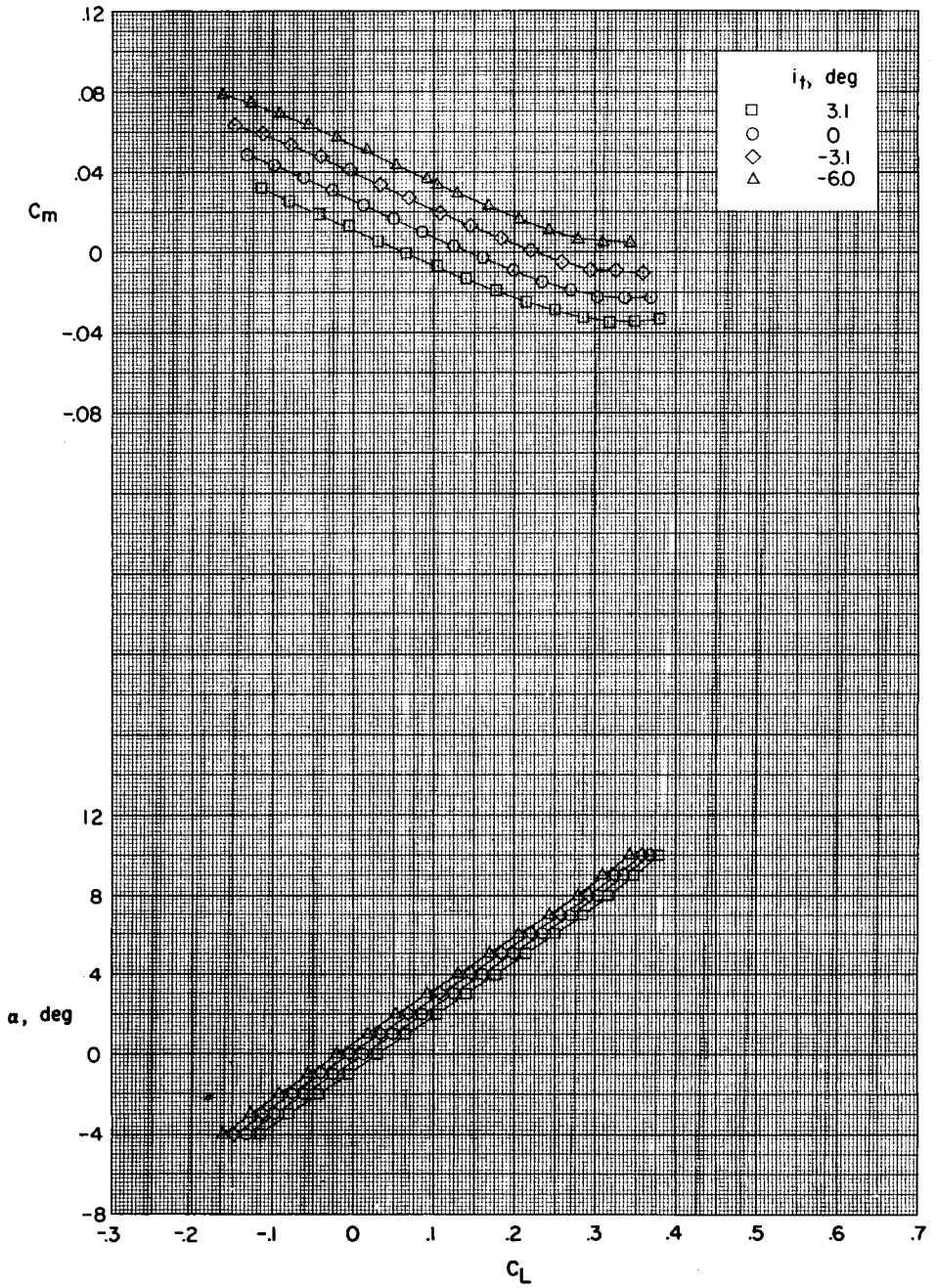

(a) Variation of pitching-moment coefficient and angle of attack with lift coefficient.

Figure 5.- Effect of horizontal tail deflection on aerodynamic characteristics in pitch for complete model with large horizontal tail.

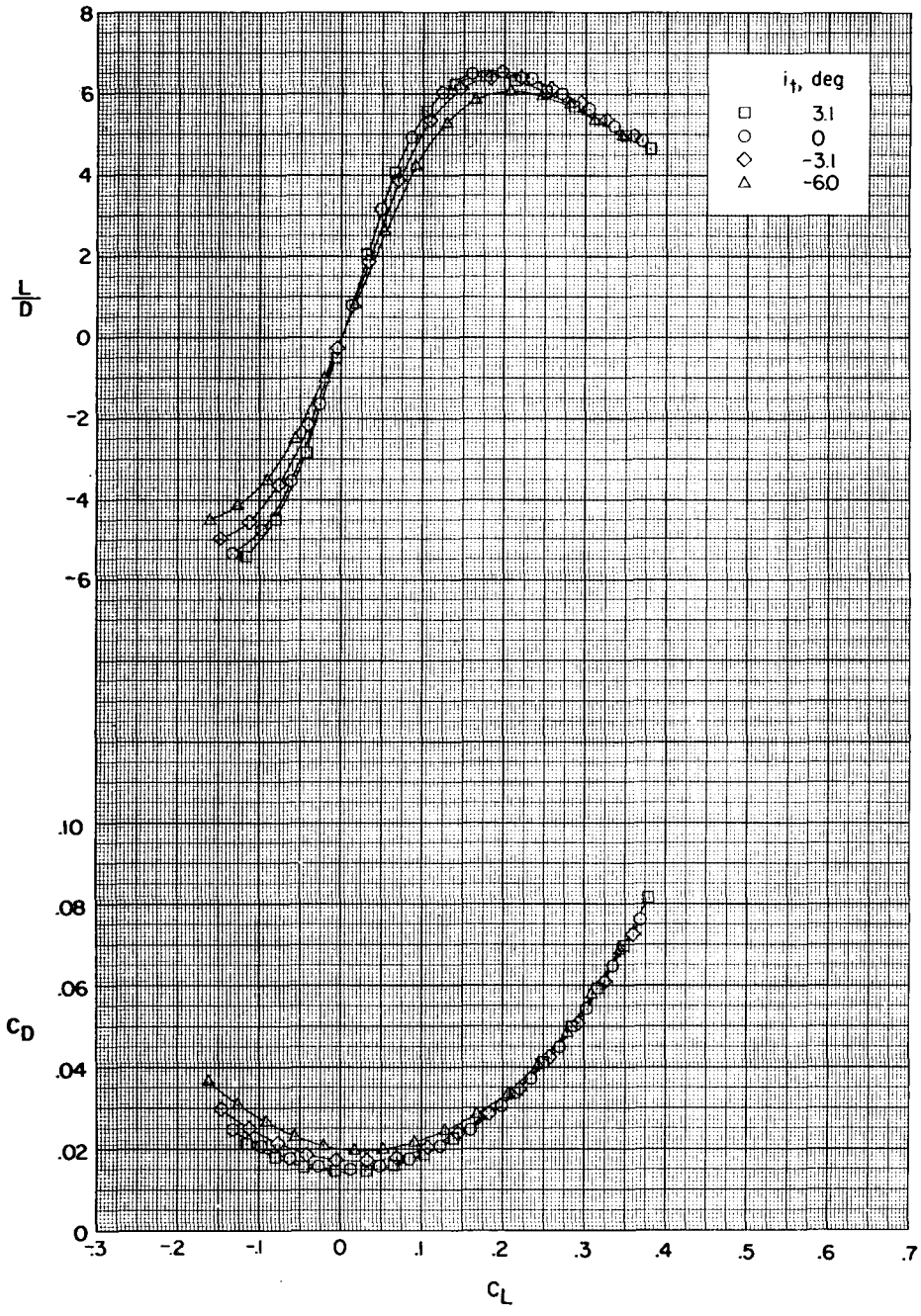

(b) Variation of lift-drag ratio and drag coefficient with lift coefficient.

Figure 5.- Concluded.

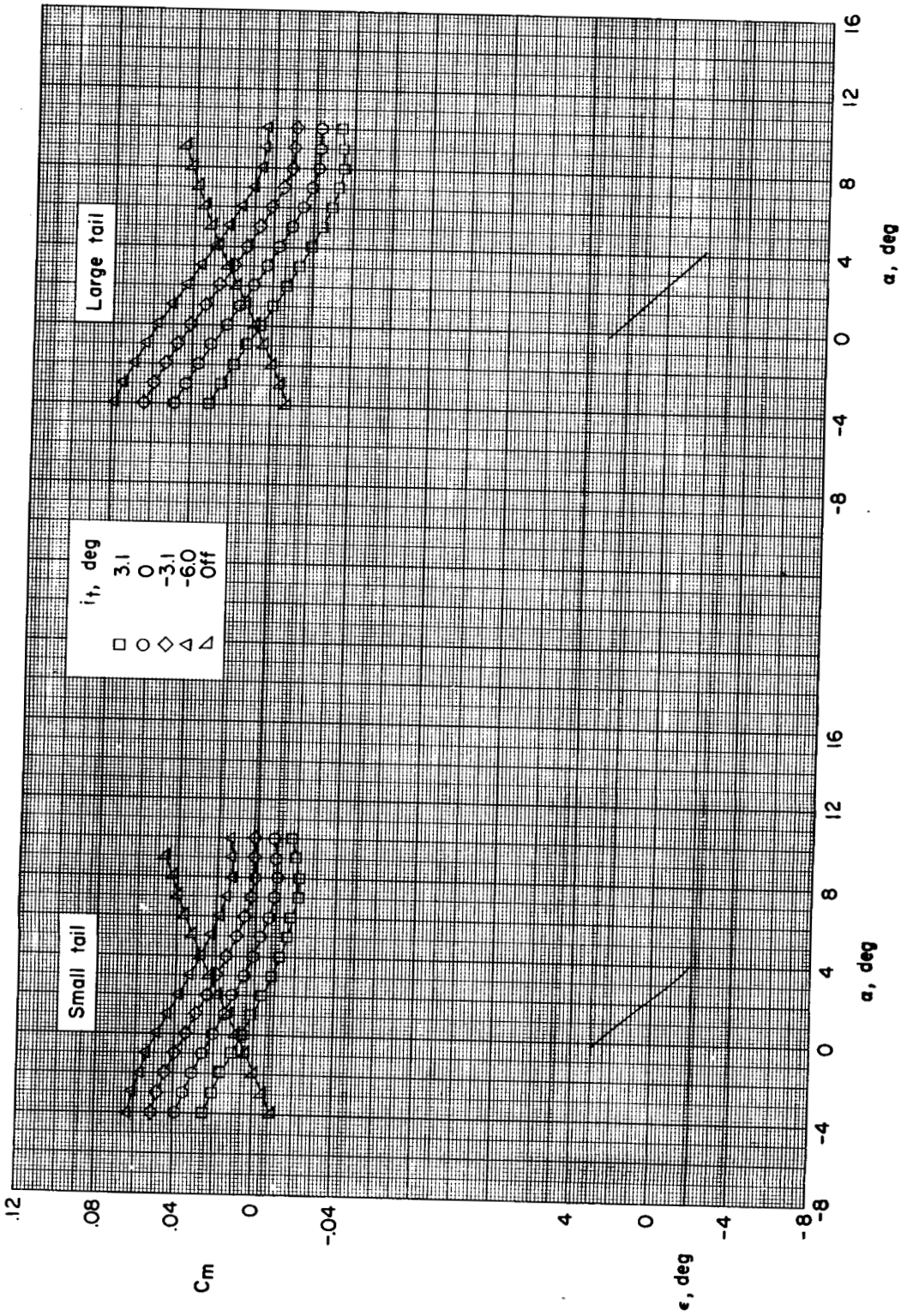

Figure 6.- Effective downwash characteristics.

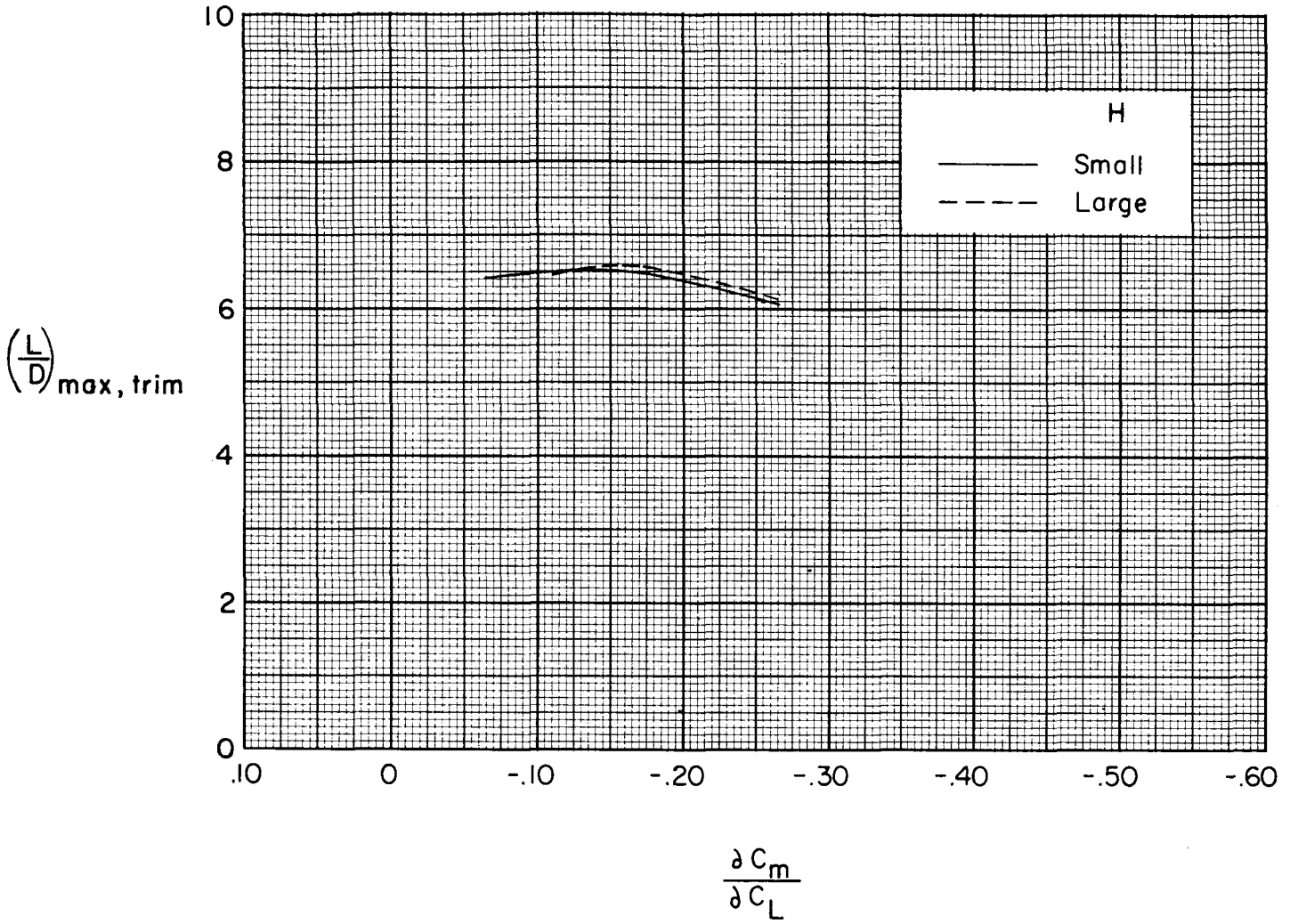

Figure 7.- Variation of trimmed maximum lift-drag ratio with longitudinal stability for complete model.

CONFIDENTIAL

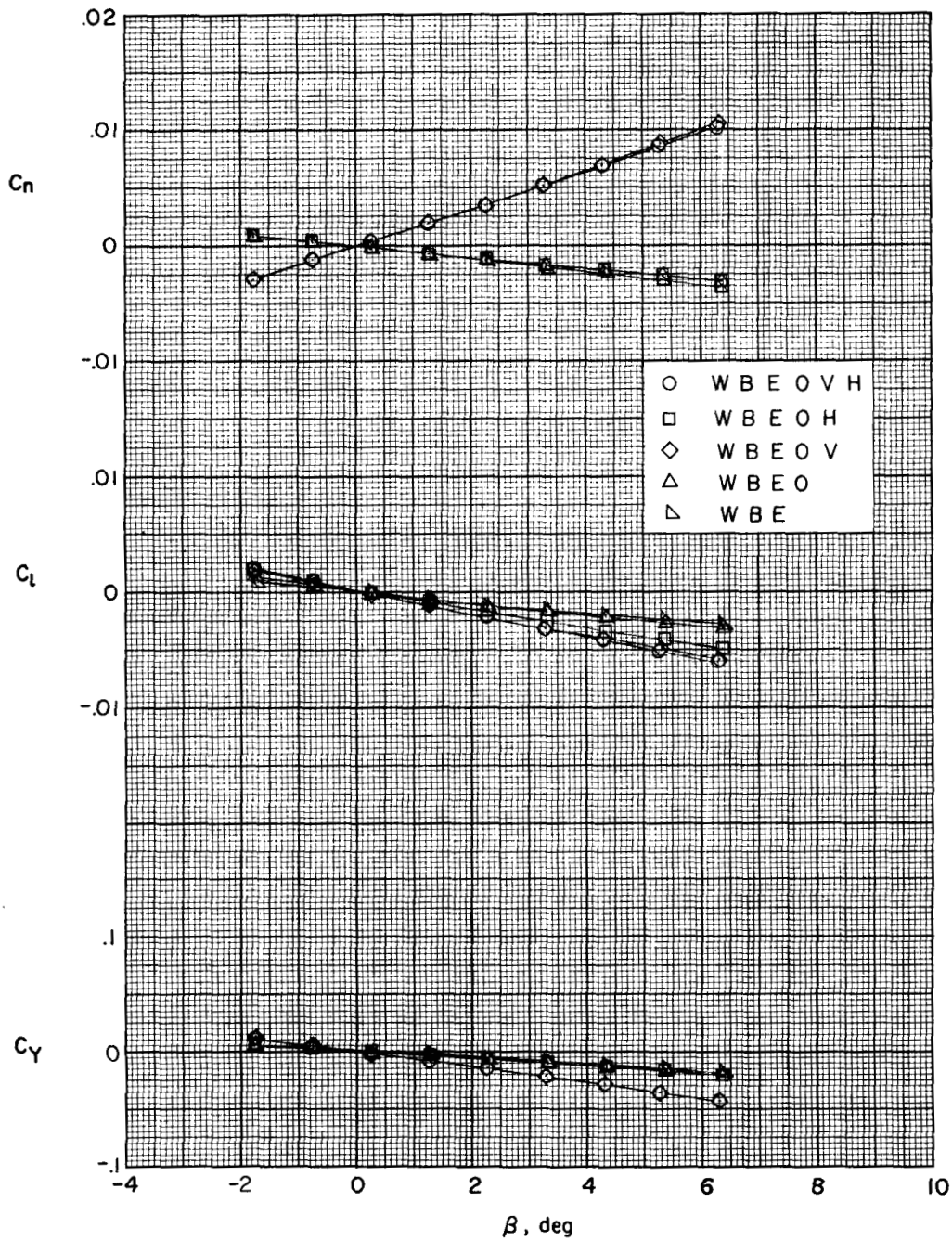

(a) $\alpha = 0^{\circ}$.

Figure 8.- Aerodynamic characteristics in sideslip for various combinations of component parts with small horizontal tail $\left(i_t = 0^{\circ}\right)$.

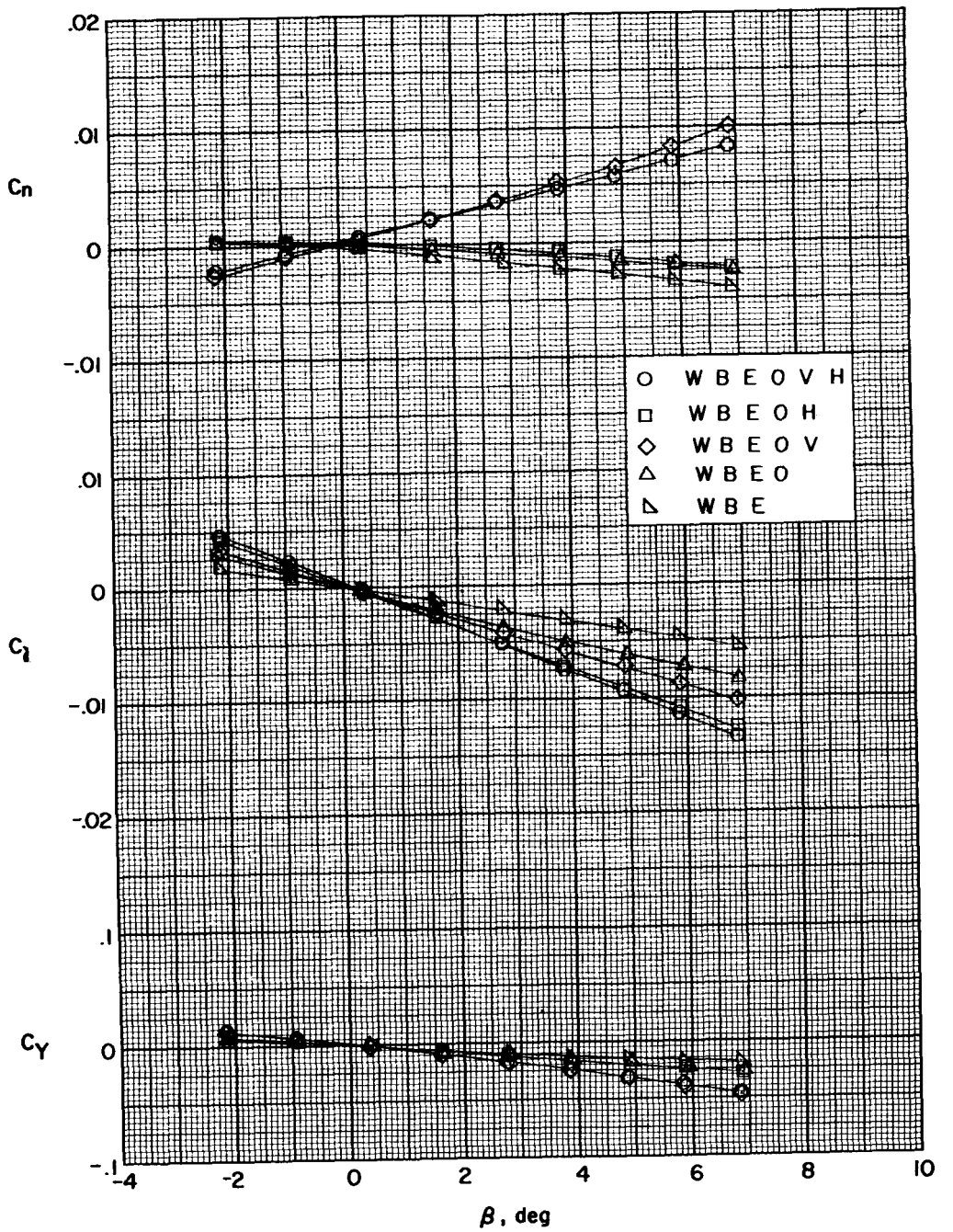

(b) $\alpha = 4^{\circ}$.

Figure 8.- Concluded.

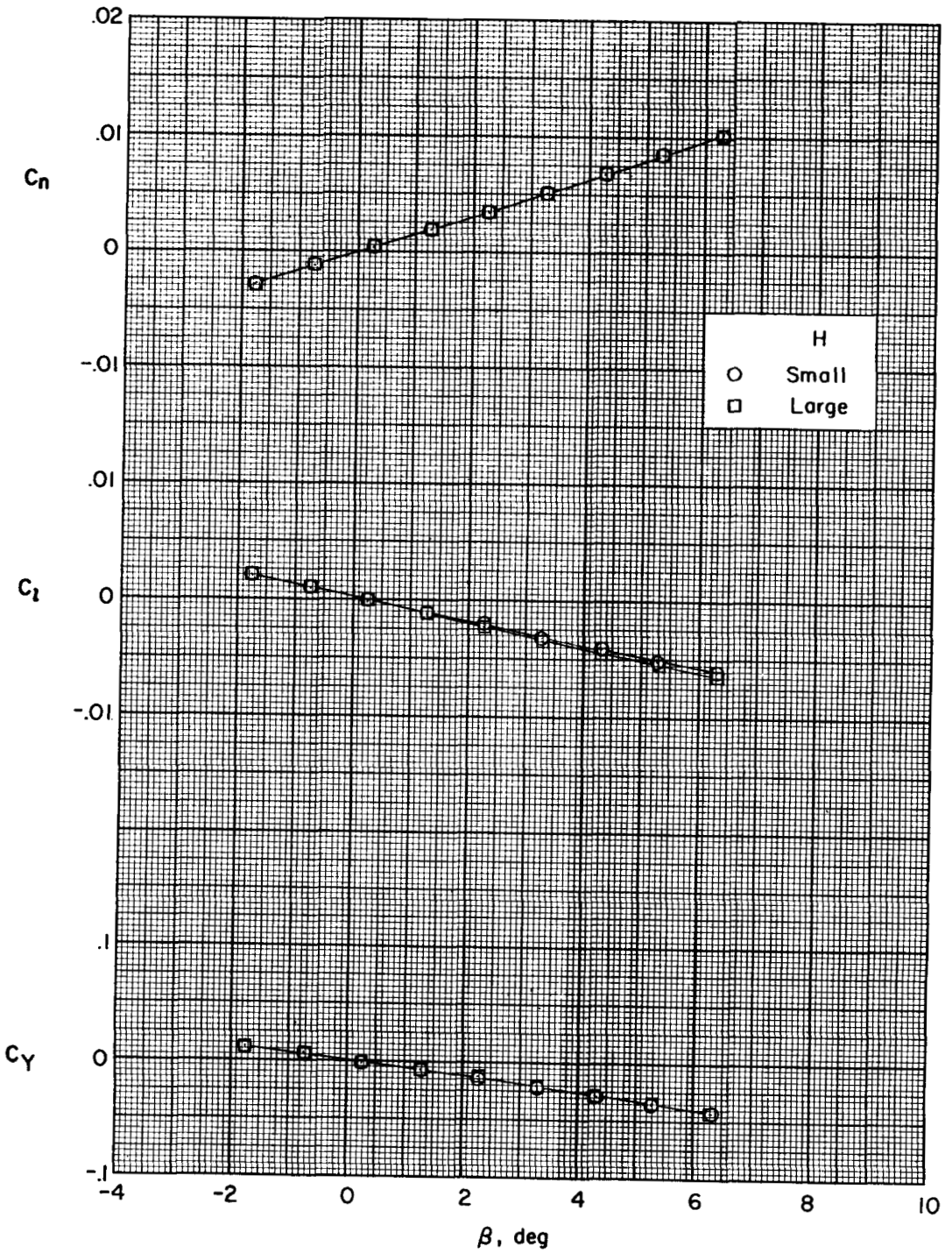

(a) $\alpha = 0^{\circ}$.

Figure 9.- Effect of horizontal tail size on aerodynamic characteristics in sideslip $\left(i_t = 0^{\circ}\right)$.

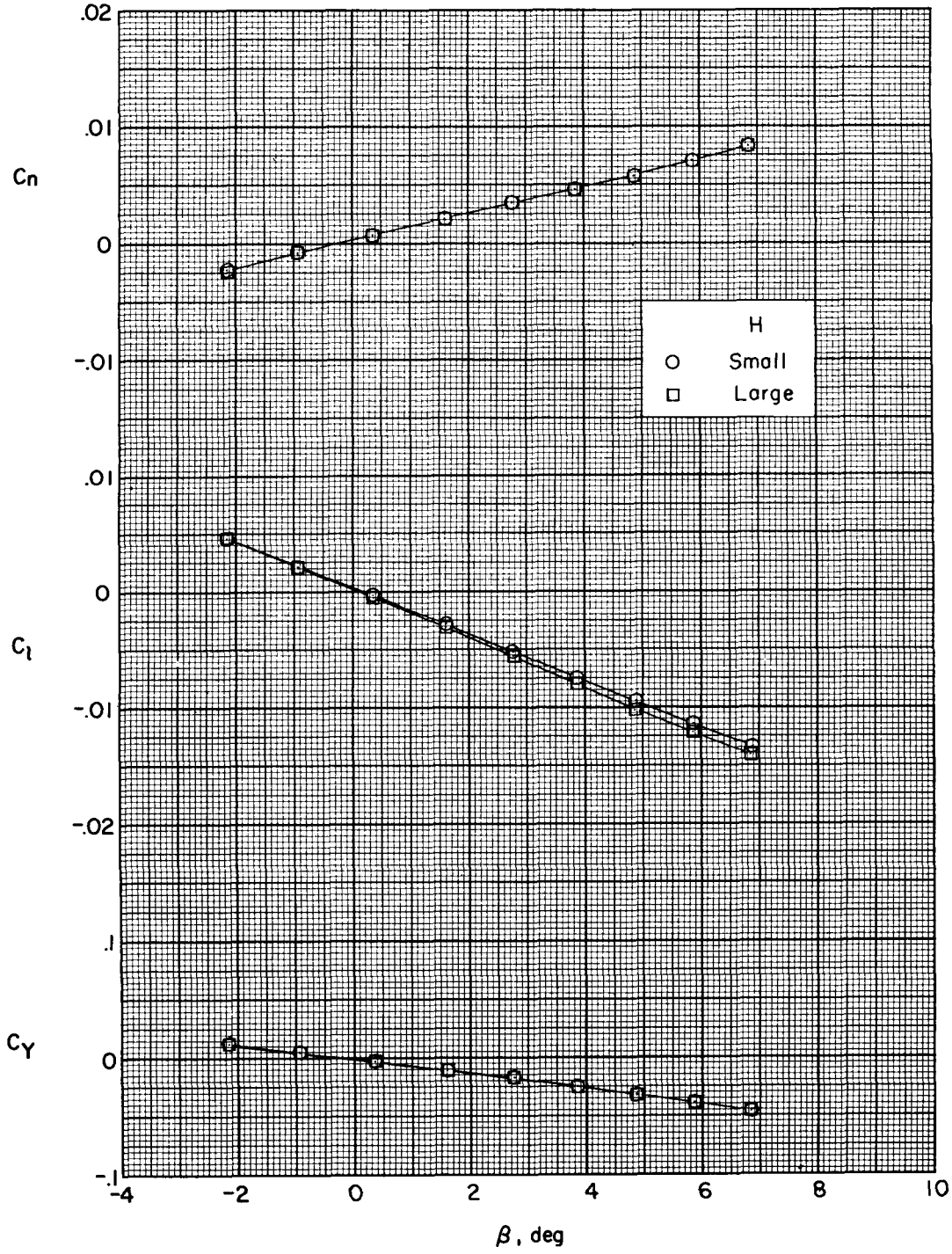

(b) $\alpha = 4^\circ$.

Figure 9.- Concluded.

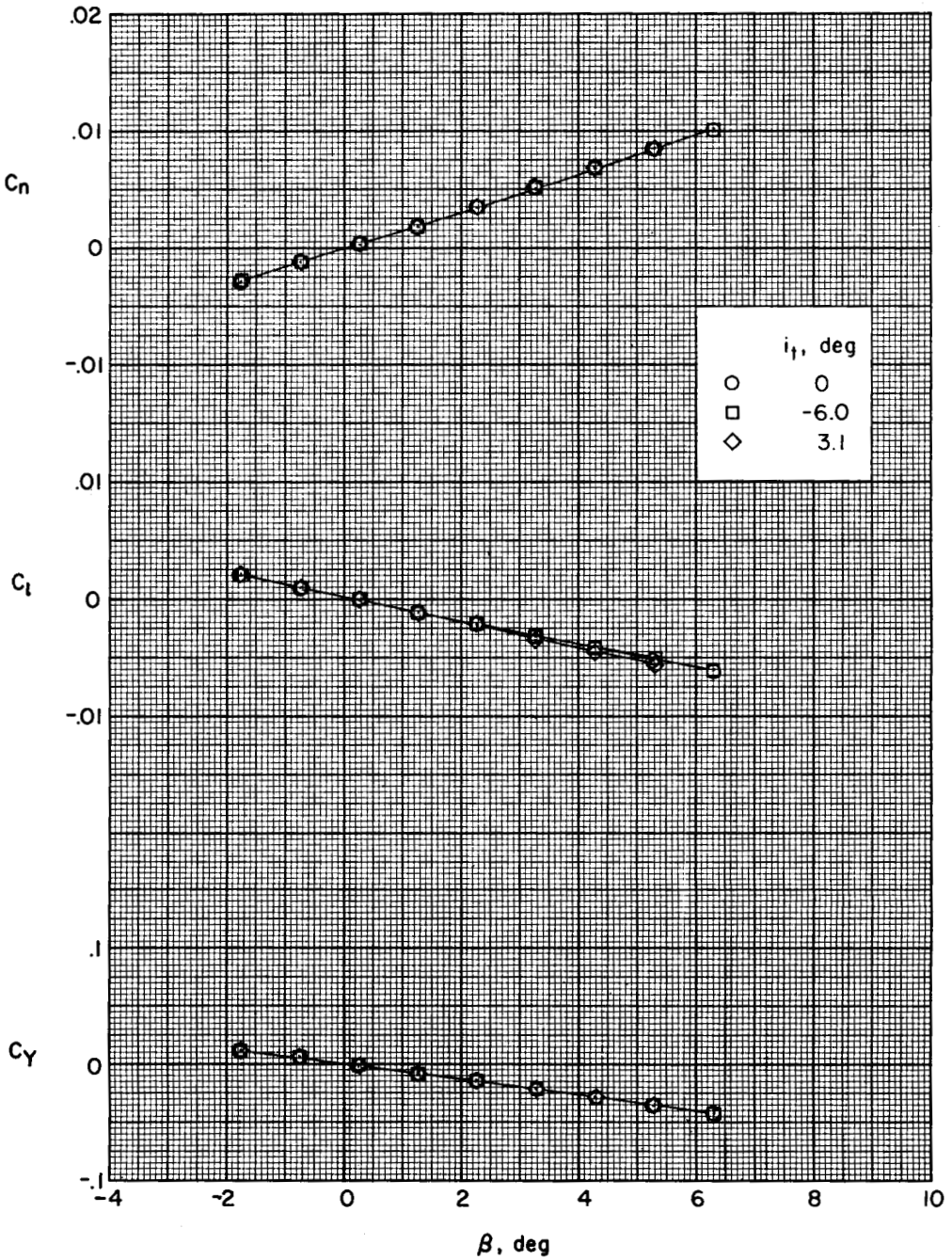

(a) $\alpha = 0^\circ$.

Figure 10.- Effect of horizontal tail deflection on aerodynamic characteristics in sideslip with small tail.

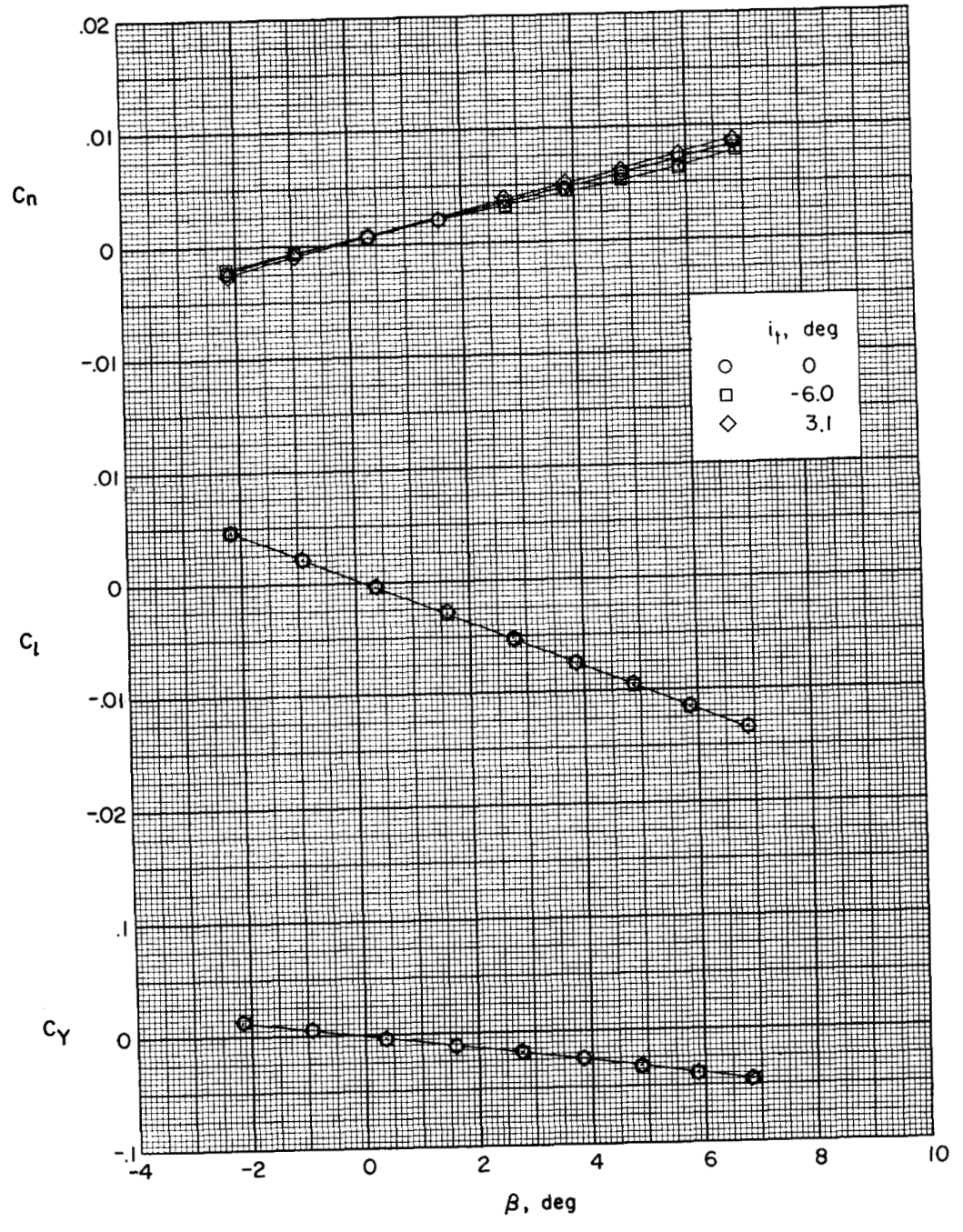

(b) $\alpha = 4^{\circ}$.

Figure 10.- Concluded.

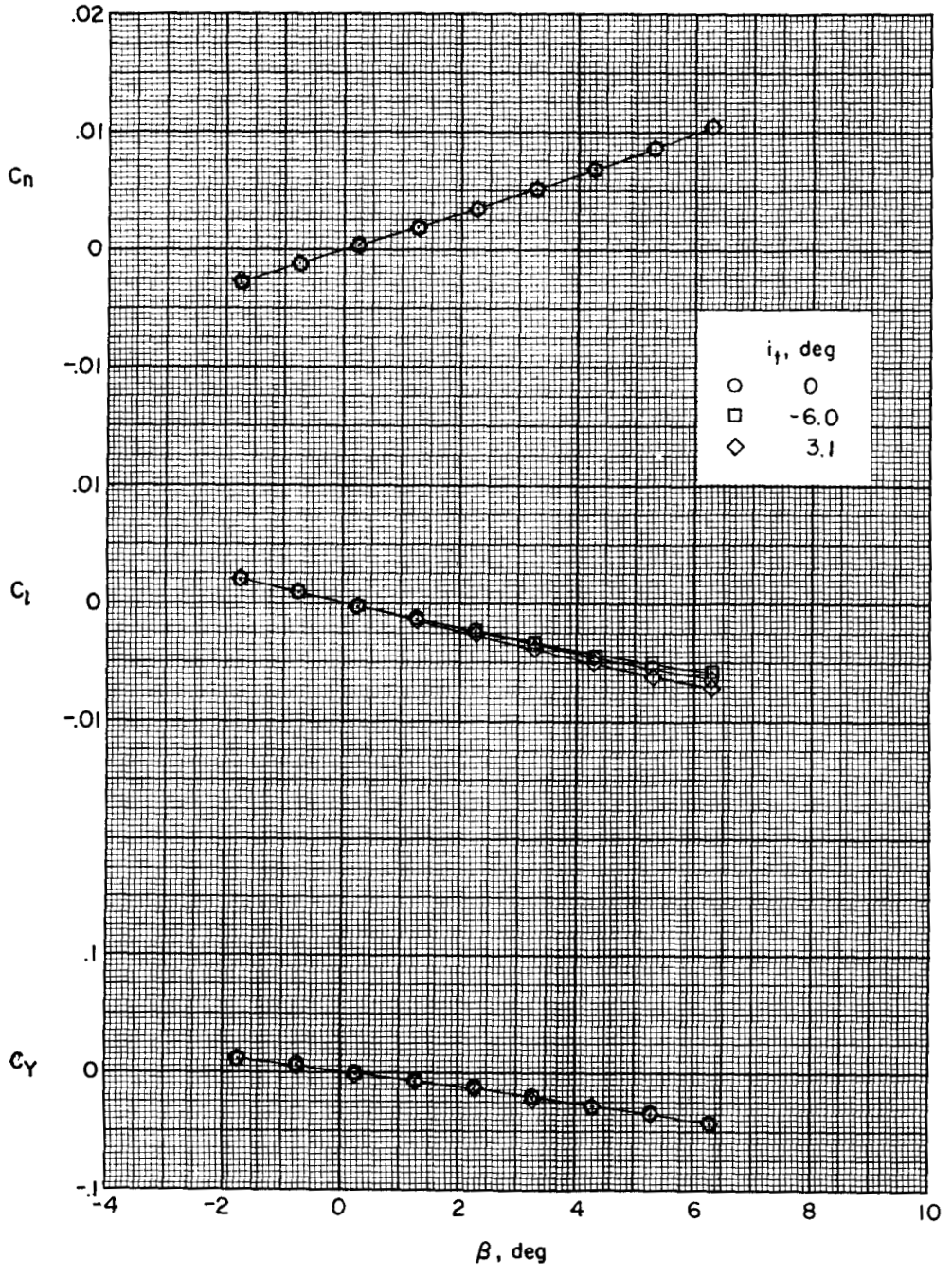

(a) $\alpha = 0^\circ$.

Figure 11.- Effect of horizontal tail deflection on aerodynamic characteristics in sideslip with large tail.

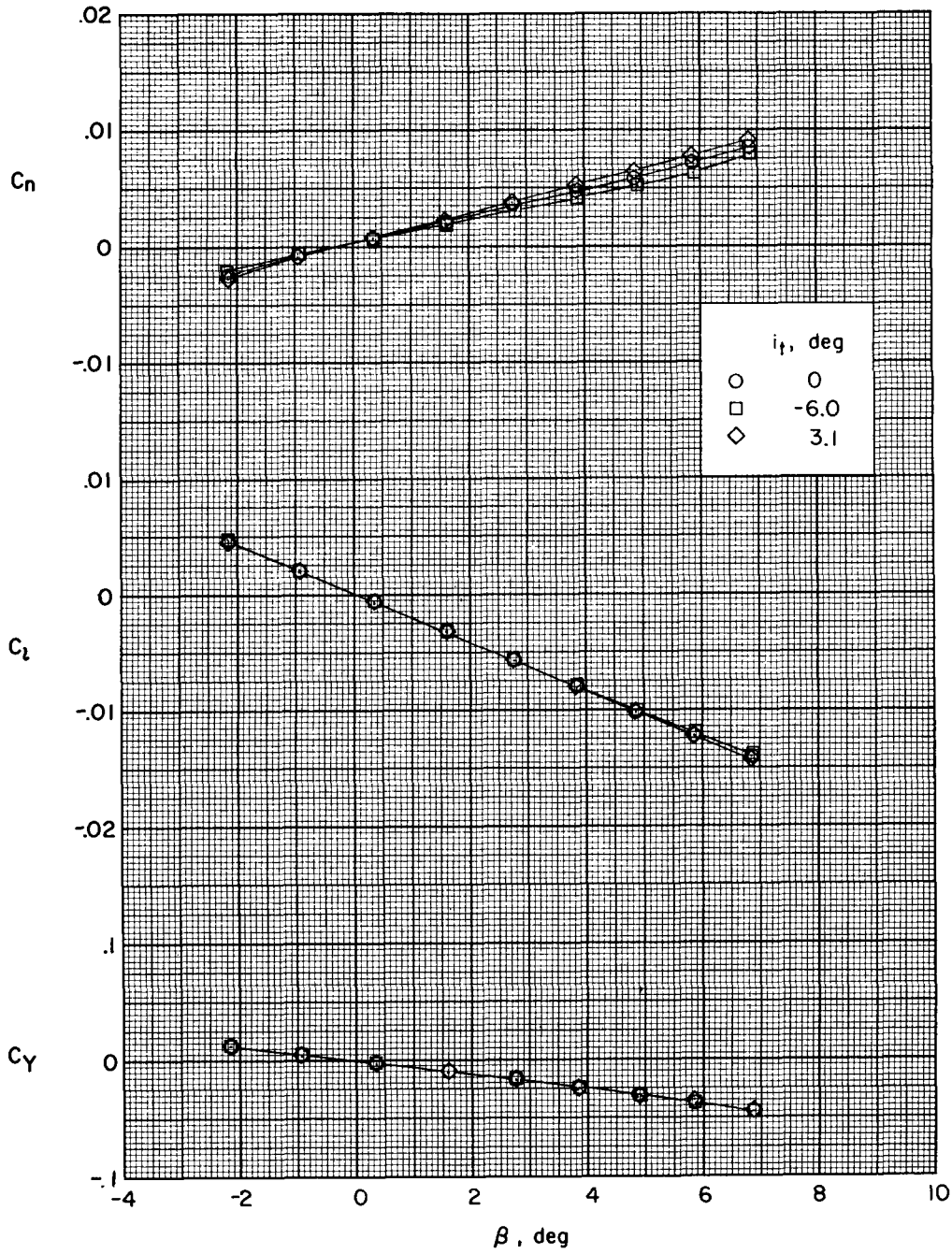

(b) $\alpha = 4^\circ$.

Figure 11.- Concluded.

NASA - Langley Field, Va. L-418